Comparative biodistribution analysis of umbilical cord mesenchymal stromal cells *via* different administration routes in rabbit models

LIANG XIAO^{1,a} CHUNLIN LIU^{2,a} YUQIAN WANG³ FUCHENG XIAO⁴ HUAJIA CAI⁵ SHOUKANG QU⁶ XIAOJUAN XU⁶ XIAOJUAN XU⁶ XIAOLIANG WANG^{6,3} YUE LIU^{6,3} YUTAO PENG³ IIA LIU^{1,6,3}*

- ¹ Department of Surgery and Oncology Shenzhen Second People's Hospital/The First Affiliated Hospital of Shenzhen University Health Science Center, Shenzhen, 518035, China
- ² Department of Interventional Therapy Shenzhen Second People's Hospital, The First Affiliated Hospital of Shenzhen University Shenzhen, China
- ³ School of Agriculture and Biotechnology, Sun Yat-Sen University, Shenzhen, Guangdong 523758, China
- ⁴ The Center of Campus, ShenZhen Senior High School Group
- ⁵ Psychiatric Medicine Sophomore, Southern Medical University
- ⁶ Shenzhen Zhongjia Biomedical Technology Co., LTD

Accepted October 18, 2025 Published online October 19, 2025

ABSTRACT

Umbilical cord mesenchymal stem cells (UC-MSCs) have shown therapeutic potential in renal diseases due to their homing ability. This study compared the effects of three administration routes (intravenous, local renal injection, and interventional injection) on UC-MSC distribution in kidney tissue. Eighteen New Zealand rabbits were assigned to the three groups (n = 6 each), and DiI-labelled UC-MSCs were tracked using confocal microscopy to evaluate their distribution in the kidney, lung, and brain. Local renal injection led to high MSC concentrations at the injection site, but distribution to the contralateral kidney was minimal and comparable to that of intravenous injection. Intravenous delivery via the marginal ear vein was simple and convenient but resulted in limited renal homing (< 1 %) and no significant difference between kidneys. Interventional injection achieved the highest delivery efficiency (12.4 %) and a more uniform renal distribution. Notably, inflammatory cytokine levels (IL-6, TNF- α , IL-10) were significantly elevated in the local injection group (p < 0.05). These results indicated that the choice of administration route critically affects MSC targeting and therapeutic potential, and interventional injection may offer the most effective strategy for precise UC-MSC delivery in renal therapy.

Keywords: delivery methods, mesenchymal stem cells, interventional therapy, renal organ, interventional procedures

INTRODUCTION

Mesenchymal stem cell (MSC) therapy is a form of regenerative medicine that utilises cellular self-renewal, immunomodulatory, anti-inflammatory, signalling, and differentiation properties to repair damaged, diseased, or injured tissues (1). MSCs function in two

^a These authors contributed equally to this work.

^{*}Correspondence; e-mail: liujia67@mail.sysu.edu.cn

ways. On the one hand, MSCs can secrete a series of paracrine factors (2, 3), which act as multi-drug "pharmacies" *in vivo*, and participate in the alleviation of pathological conditions through anti-inflammatory, anti-apoptotic, and immunomodulatory mechanisms (4). On the other hand, their inherent pluripotency and differentiation potential offer therapeutic options for a variety of diseases. In recent years, the incidence and lethality of renal diseases have been increasing, posing a serious threat to human health. Renal diseases are among the leading causes of death globally, with an estimated 1.43 million deaths in 2019. The burden of renal diseases has increased over time compared to other noncommunicable diseases (5). To date, it is difficult to obtain satisfactory therapeutic effects with traditional treatment modalities.

MSCs have been recognised as effective and safe treatments for renal diseases in preclinical and clinical studies, and have played an active role in the treatment of several types of renal disease. For example, the conditioned media derived from MSCs (MSC-CM) attenuates experimental anti-glomerular basement membrane glomerulonephritis through M2 macrophage-mediated anti-inflammatory effects (6). In systemic lupus erythematosus, transplantation of allogeneic MSCs reduces kidney injury (7). One clinical trial has also shown that treating patients with systemic lupus erythematosus using allogeneic MSCs from healthy donors is both safe and feasible (8). In a model of Adriamycininduced nephrotic syndrome, MSCs exert their therapeutic effect mainly by modulating inflammation (9). Moreover, patients with idiopathic nephrotic syndrome (INS) have been treated with autologous MSC infusions (10). In a Thy1.1 antibody-induced rat glomerulonephritis model, hypoxia-pretreated MSCs reduced glomerular apoptosis, autophagy, and inflammation through HIF- 1α /VEGF/Nrf2 signalling (11).

Notably, MSCs can also inhibit inflammatory factors in nephritis. For instance, in focal segmental glomerulosclerosis, MSCs reduce circulating inflammatory factors and improve renal function (12). Meanwhile, autologous MSCs have been applied to treat anti-neutrophil cytoplasmic antibody-associated vasculitis (13) and autosomal dominant polycystic kidney disease (14), with no reported clinical or serious adverse events. In addition, existing studies have also proposed that MSCs may alleviate focal segmental glomerulosclerosis through the regulation of IL-22. The above-mentioned animal models and clinical trials provide substantial evidence for the therapeutic potential of MSCs in the treatment of renal diseases. In brief, MSCs demonstrate great potential to localise to damaged kidneys and promote both morphological and functional recovery.

Migration to the site of tissue injury is the first step in stem cell-mediated tissue regeneration. The homing of MSCs in injured tissues is dependent on their ability to migrate to and interact with the local micro-environment, thus ensuring that they are anchored at locations where their effector functions are required (15). It is important to achieve cellular homogeneity, ensure cell survival, and maintain high implantation efficiency during local or systemic administration (16). However, different routes of drug delivery can affect the distribution (17), survival and therapeutic effects of MSCs. Therefore, choosing the appropriate mode of drug delivery is crucial for the effectiveness of MSC treatment.

It is widely known that tail vein injection is one of the most commonly used modes of MSC drug delivery (18). Numerous rodent modelling experiments have demonstrated its effectiveness. For example, tail vein infusion of MSCs in mice with ischemia—reperfusion kidney injury resulted in decreased serum creatinine and urea nitrogen levels, along with amelioration of tubular injury (19). Specifically, activation of two mitogen-activated pro-

tein kinases, p38 and ERK, is inhibited; expression of Bax and cleaved caspase-3 is down-regulated; and expression of Bcl-2 is up-regulated by intravenous infusion of MSCs in rats with cisplatin-induced acute kidney injury, which protects renal function and structure by inhibiting apoptosis (20). However, *in vivo* imaging confirmed that a large number of MSCs were present in the lungs and spleen, and only a small number of MSCs were found in the kidneys (21).

It is noteworthy that localised injection involves delivering cells directly into the kidney under ultrasound guidance, allowing them to remain within a "closed" zone (22). For example, in a beagle dog model of cisplatin-induced acute kidney injury, localised injection of MSCs led to decreased serum creatinine and urea nitrogen levels, prolonged survival time, and the presence of MSCs near the renal tubules was confirmed (23). Another study in cats with chronic kidney injury reported a slight improvement in glomerular filtration rate and a corresponding decrease in serum creatinine concentration following MSC treatment. However, the need for extensive sedation and invasive procedures to perform localised injection presents a significant barrier to its clinical application (24).

Interventional target-organ arterial drug delivery is an emerging therapeutic method that lies between surgical and medical treatments (25). A guide wire is inserted into the femoral artery, and the drug is delivered directly to the target site under angiographic guidance, which improves the concentration of the drug at the target site and reduces the dosage of the drug and its side effects (26). In stem cell therapy, interventional approaches have also been explored to improve targeted cell delivery. For example, to minimise the risk of pulmonary complications due to MSC entrapment in the lungs following systemic infusion, cells were administered distally *via* the thoracic aorta. This strategy avoided respiratory distress, and no serious adverse events were observed during a 6-month follow-up period (27). The clinical therapeutic efficacy of MSCs has always been in the spotlight, and little attention has been paid to the impact of different cell delivery routes on delivery efficiency. In addition, interventional target organ arterial drug delivery in rodent models has not been reported due to the limitation of their body size, which makes it difficult to perform femoral artery puncture surgery (28). Therefore, rabbits, which are larger than typical rodents, were selected as the experimental subjects in this study.

To examine which delivery route was most suitable for MSC delivery, Dil fluorescent dye-labelled cells were first injected into experimental rabbits through different delivery routes. Afterwards, the delivery efficiency of the cells was relatively quantified according to the percentage of fluorescent cells in the kidney cross-section area, and compared by evaluating the effects of the three different delivery routes on MSC aggregation targeting the kidneys. This study aims to provide a reference for choosing the optimal injection route for MSC delivery in subsequent preclinical and clinical trials.

EXPERIMENTAL

Animals

Twelve-week-old New Zealand white rabbits (weighing 2–2.5 kg) were purchased from Shandong Shaoda Breeding Co., Ltd. (China). The animals were housed in the animal facility of Shenzhen Zhongjia Bio-Medical Technology Co., Ltd. under standard condi-

tions: temperature of 25 ± 3 °C, a 12 h light/dark cycle, and free access to food and water. All animal procedures were performed in accordance with the ethical guidelines for laboratory animal welfare and conformed to the "Administrative Measures for Laboratory Animal Permits" and the "Regulations on the Administration of Laboratory Animals". The experimental protocol was approved by the Animal Ethics Committee (approval number: BG-AMS-20240314LN01-Y).

Cells

Human umbilical cord-derived mesenchymal stem cells (UC-MSCs) were obtained from Shenzhen Zhongjia Bio-Medical Technology Co., Ltd. The cells were used for fluorescent labelling and injection experiments as described in subsequent sections.

Reagents and instruments

Dil cell fluorescent dye and wheat germ agglutinin (WGA) were obtained from Solepol (China). The anti-fade mounting medium and DAPI were purchased from MedChemExpress (USA). The 4 % paraformaldehyde solution was purchased from Sigma-Aldrich (USA). TNF- α , IL-6, IL-10, and GAPDH primers were sourced from Sangon Biotech (China). The EasyScript® First-Strand cDNA Synthesis SuperMix and TransStart® TopGreen qPCR SuperMix were obtained from TransGen Biotech (China).

The confocal microscope (A1HD25, Nikon, Japan), cryostat (CryoStar NX70, Thermo Fisher Scientific, USA), NanoDrop Microvolume Spectrophotometer (Thermo Fisher Scientific), and PCR machine (Thermo Fisher Scientific) were used for the experiments. The slide scanner was purchased from Shengqiang Technology Co., Ltd. (China). The Biomapping 9000 system was provided by Wuhan Woyi Biotechnology Co., Ltd. (China).

UC-MSCs culture procedure

UC-MSCs were thawed in a 40 °C water bath and immediately transferred into precooled (4 °C) sterile saline. After gentle mixing, the cells were centrifuged at $500 \times g$ for 5 min to remove cryoprotectant. The cell pellet was washed twice with sterile saline, resuspended in complete growth medium, and seeded into T175 flasks. Cultures were maintained at 37 °C in a humidified incubator with 5 % CO₂. The medium was replaced every 2–3 days. When cells reached 80–90 % confluency, they were passaged using 0.25 % trypsin-EDTA. Cells were either expanded for further experiments or cryopreserved (29).

UC-MSCs cell staining

To prepare fluorescently labelled UC-MSCs for injection, 1×10^7 cells were incubated with 10 mL of 10 μg mL⁻¹ DiI red fluorescent membrane dye (Solepol) at room temperature for 10 min with gentle mixing every 5 min. Cells were centrifuged at $500 \times g$ for 5 min, washed twice with sterile saline, and resuspended in saline to obtain suspensions at the required concentrations for injection. In parallel, another aliquot of 1×10^7 UC-MSCs was incubated with 4 mL of 10 μg mL⁻¹ WGA green fluorescent membrane dye (Solepol) at room temperature for 30 min with mixing every 5 min, followed by two washes by centrif-

ugation under the same conditions. Cell viability post-labelling exceeded 95 % as confirmed by the trypan blue exclusion assay.

UC-MSCs administration

Labelled UC-MSCs were administered to the rabbits via the marginal vein of the ear, *via* the interventional left renal artery, and via the localised direct injection of the left kidney.

- (i) Trans-interventional left renal artery administration: rabbits were anaesthetized using 20 % urethane (Yanni, 2004) (750 mg kg⁻¹) by intraperitoneal injection, and a fixed indwelling needle in the marginal ear vein was used for intraoperative supplementation with 0.9 % saline and 20 % urethane to maintain the anaesthesia. The rabbit was dorsalized at the groin of the hind limb, and the skin was opened to expose the femoral artery. A guidewire was inserted from the femoral artery to reach the left renal artery of the left kidney, and then the location of the guidewire was determined by contrast angiography. Each rabbit was injected with 4 mL of 8×10⁶ red fluorescent-labelled MSCs.
- (ii) Localised direct injection in the left kidney: First, the location of the kidney was visualised by ultrasound imaging on the skin behind the left kidney of the rabbit. Then, the needle of the syringe was guided to the cortex of the left kidney. Each rabbit was injected with 1.5 mL of 8×10^6 red fluorescently labelled UC-MSCs.
- (iii) Marginal ear vein injection: the rabbits were immobilised. The skin was prepared at the ear marginal vein, and alcohol was swabbed to expose the blood vessels. Each rabbit was injected with 4 mL of 8×10^6 red fluorescently labelled UC-MSCs. A dry cotton ball was pressed to stop bleeding.

Renal tissue immunofluorescence staining

Kidney-frozen sections were obtained between 12 and 24 h after cell injection. Euthanasia was performed on rabbits by injecting 20 mL of air through a marginal ear vein, and frozen sections were made from the kidneys, lungs, and cerebral hippocampus. The renal peritoneum was peeled off, and transverse sections were made along the middle of the kidney. The tissues were embedded in optimal cutting temperature compound and frozen in a –20 °C cryostat. Sections were cut at a thickness of 6 μm . The sections were fixed by dropwise addition of 200 μL of 4 % paraformaldehyde for 15 min, washed three times with PBS-T (PBS containing 0.1 % Tween 20) for 3 min each time, and stained with DAPI for 15 min. DAPI was discarded, and the slices were blocked by dropwise addition of 20 μL of anti-fluorescent bursting agent. Fluorescence images were captured by confocal laser scanning microscopy (Olympus, Germany).

Real-time fluorescence quantitative PCR

Kidney tissues from both ends of the organ were collected from rabbits in each group for real-time fluorescence quantitative PCR (qPCR) analysis. The procedure involved the following steps: A suitable amount of kidney tissue was placed in a 1.5 mL centrifuge tube containing 1 mL of Trizol reagent and then homogenised using a high-speed tissue grinder. RNA was subsequently extracted using chloroform and isopropanol. Reverse transcription was carried out using the EasyScript® First-Strand cDNA Synthesis SuperMix Kit, following the manufacturer's protocol for reaction system setup and program settings. The

resulting cDNA was then analyzed *via* real-time fluorescence qPCR using the TransStart® TopGreen qPCR SuperMix Kit, with qPCR performed according to the kit instructions to quantify target gene expression levels.

Laser confocal microscope imaging

Confocal laser scanning microscopy was performed using a 10× objective lens with bidirectional scanning at a speed setting of 4.8 and a resolution of 1024×1024 pixels. A 5×5 tile scan was applied for image stitching. The DAPI channel was detected with excitation/emission wavelengths of 360/470 nm, while the Dil channel was detected at 549/565 nm.

Biomapping processes

Freshly excised kidneys were fixed in 4 % paraformaldehyde (tissue-to-fixative ratio 1:3, V/V) at 4 °C for 24 h. Prior to imaging, the samples were mounted on a three-dimensional (3D) panning platform and immersed in 0.01 mol L⁻¹ phosphate-buffered saline (PBS) to enhance wheat germ agglutinin (WGA) fluorescence. Light-sheet imaging was performed using a Biomapping 9000 microscopy system, applying a tomographic imaging strategy with a physical section thickness of 40 μ m and excitation/emission wavelengths of 491/516 nm. The imaging process consisted of four sequential steps: (i) sectioning with a vibrating blade at 77 Hz and a slicing speed of 0.2 mm s⁻¹; (ii) positioning of the platform at the imaging start point; (iii) light-sheet scanning for image acquisition; and (iv) returning the platform to the preset position in preparation for the next imaging cycle (30).

Data analysis

Cell distribution in the cross-sectional images was quantified using ImageJ software. Specifically, the total number of nuclei stained by DAPI (x) and the number of cells co-stained with DAPI and Dil (y) within each field of view were counted. The proportion of red fluorescently labelled cells was calculated using the formula: N = (x - y) / x. Statistical analyses were performed using Prism 8 software.

RESULTS AND DISCUSSION

Homing of UC-MSCs to the target organs

The UC-MSCs delivery efficiency of different injection routes for the homing or localisation of UC-MSCs to the target organs varied (Fig. 1). The delivery efficiency of UC-MSCs to the target organs varied depending on the injection route (Fig. 1). Notably, in the localised injection mode, UC-MSCs were predominantly concentrated at the injection site within the left kidney cross-section. Specifically, in the localised injection group, UC-MSCs were mainly confined to the injection region (28.4 %, Fig. 1b), which accounted for only one-quarter of the total left kidney cross-sectional area. Accordingly, calculations indicated that UC-MSCs in this treatment represented 7.1 % of the entire left kidney cross-sectional area (Fig. 1d). In contrast, other injection routes showed a more uniform cell distribution, requiring no additional computation. Intravenous injection resulted in the lowest number of red

fluorescently labeled cells in the left kidney cross-section, accounting for less than 1 % (Fig. 1c), whereas the interventional injection route yielded the highest number, reaching up to 12.4 % (Fig. 1a). This difference is likely due to the fact that interventional delivery via the left renal artery effectively enhances UC-MSCs targeting efficiency: the cells first pass through the target kidney *via* the artery, where they are captured by small blood vessels, extravasate, and colonize, allowing a large number of cells to reach the target organ. Localised injection can "seal" a substantial number of cells at the injection site. In contrast, intravenous administration results in only a small fraction of cells reaching the target organ through systemic circulation, with the majority being lost during circulation.

In contrast to the obvious difference in the left kidney, no statistically significant difference between the three injection modalities was shown in the laser confocal microscopy

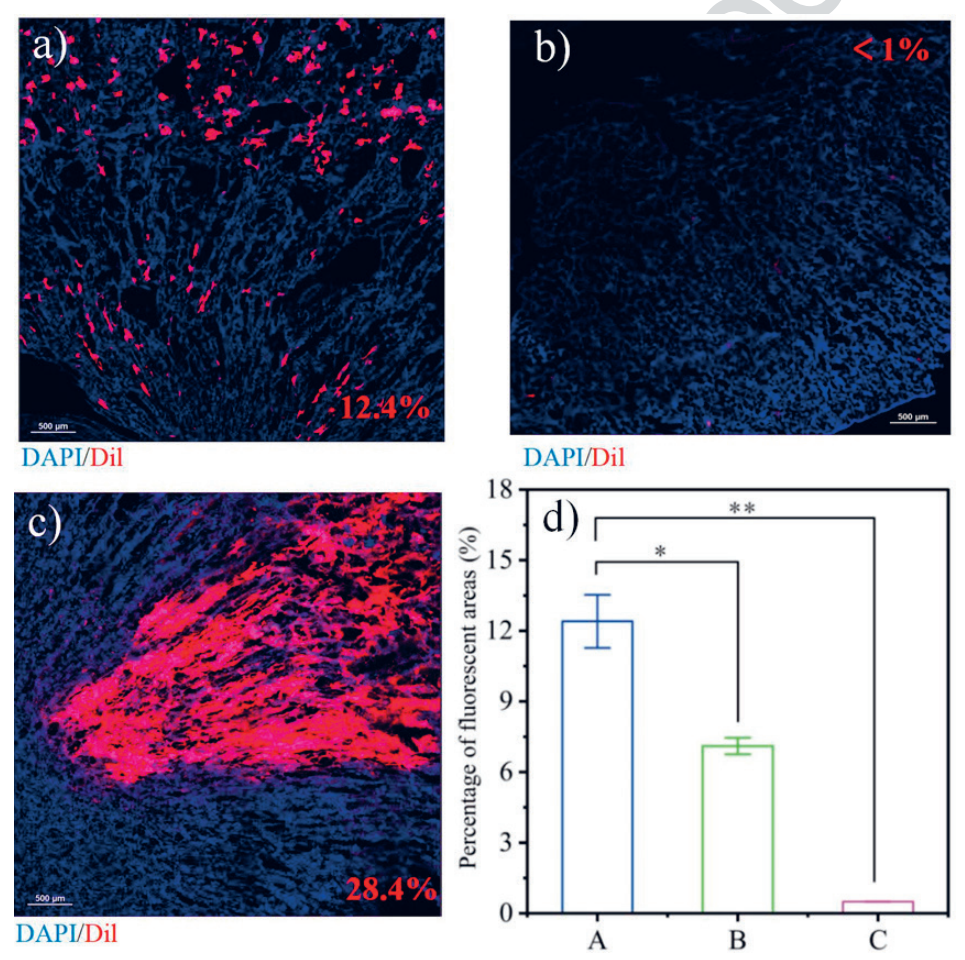


Fig. 1. Differences in the distribution of labelled UC-MSCs in the cross-sections of the left kidney of rabbits from different groups: a) interventional injection; b) localised injection zone; c) intravenous injection; d) percentage of fluorescent areas. * p < 0.05, ** p < 0.01.

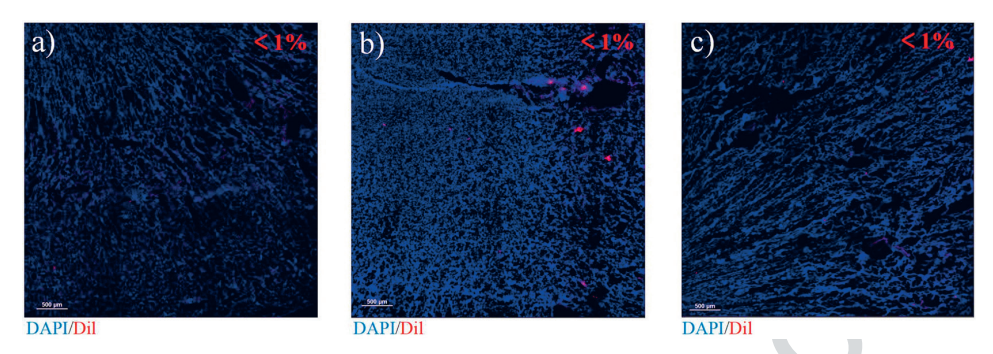


Fig. 2. Differences in the distribution of labelled UC-MSCs in the cross-section of the right kidney: a) interventional injection; b) localised injection; c) intravenous injection.

imaging results of the right kidney cross-section. The number of red fluorescently labeled cells distributed in the cross-section of the right kidney was < 1 % for the interventional injection (Fig. 2a), the localized injection (Fig. 2b), and the intravenous injection (Fig. 2c). It was found that there was a large difference in the number of cells distributed in the left and right kidneys of the same individual. A considerable number of cells were intercepted by the left renal microvessels in the interventional left renal artery administration mode, and some of the cells continued to participate in the systemic circulation, allowing red fluorescently labelled cells to also be detected in the contralateral kidney (31). In addition, cells could not only spill over into the tissues through the blood vessels but also re-enter the blood vessels from the tissue mesenchyme, which then circulated throughout the body and was detected in the contralateral kidney (4).

Impacts of UC-MSCs treatment on inflammatory cytokine expression

RT-qPCR was used to analyze the gene expression of the pro-inflammatory cytokines TNF- α and IL-6, as well as the anti-inflammatory cytokine IL-10 (Fig. 3). the localized

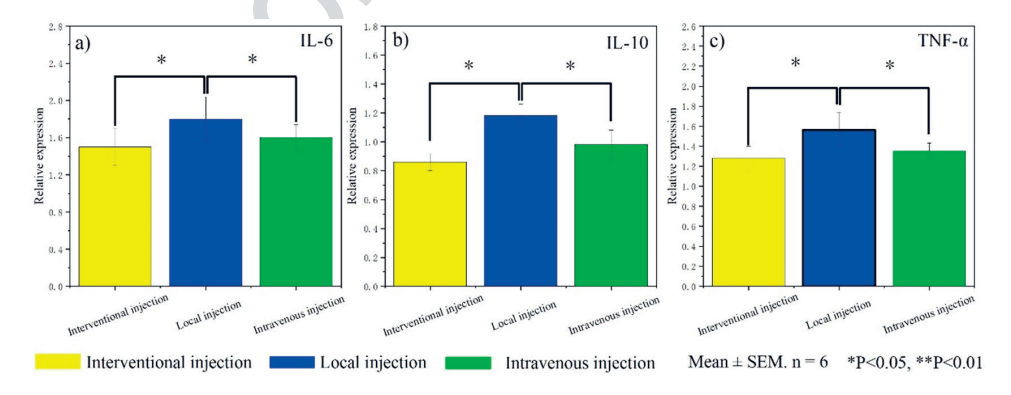


Fig. 3. Relative mRNA expression levels of a) TNF- α , b) IL-6, and c) IL-10 in the left kidneys from each group. Mean \pm SEM, n = 6. * p < 0.05.

injection group exhibited a significant increase in both IL-6 and TNF- α expression (p < 0.05), as well as in IL-10 expression (p < 0.05), suggesting that localized injection may influence the inflammatory response, potentially through elevated chemokines and immunosuppressive factors. Additionally, the expression levels of IL-6, IL-10, and TNF- α in the interventional group were comparable to those in the intravenous interventional injection groups (p < 0.05). These results suggest that there was a lower level of inflammation in the intravenous and interventional injection groups as compared to the localised injection group. IL-6, TNF- α , and IL-10 are key markers of the inflammatory response, and their expression was significantly altered following UC-MSCs treatment, likely due to the potent immunomodulatory functions and multipotency of UC-MSCs.

Distribution of UC-MSCs in the kidney via interventional delivery

In previous studies, interventional methods were predominantly applied for cancer-targeted drug delivery (32). In this study, UC-MSCs were applied to the New Zealand rabbit model for the first time via interventional left renal artery administration. Conventionally, MSCs were delivered either locally or intravenously, but these approaches resulted in substantial cell loss during systemic circulation, with only a small proportion

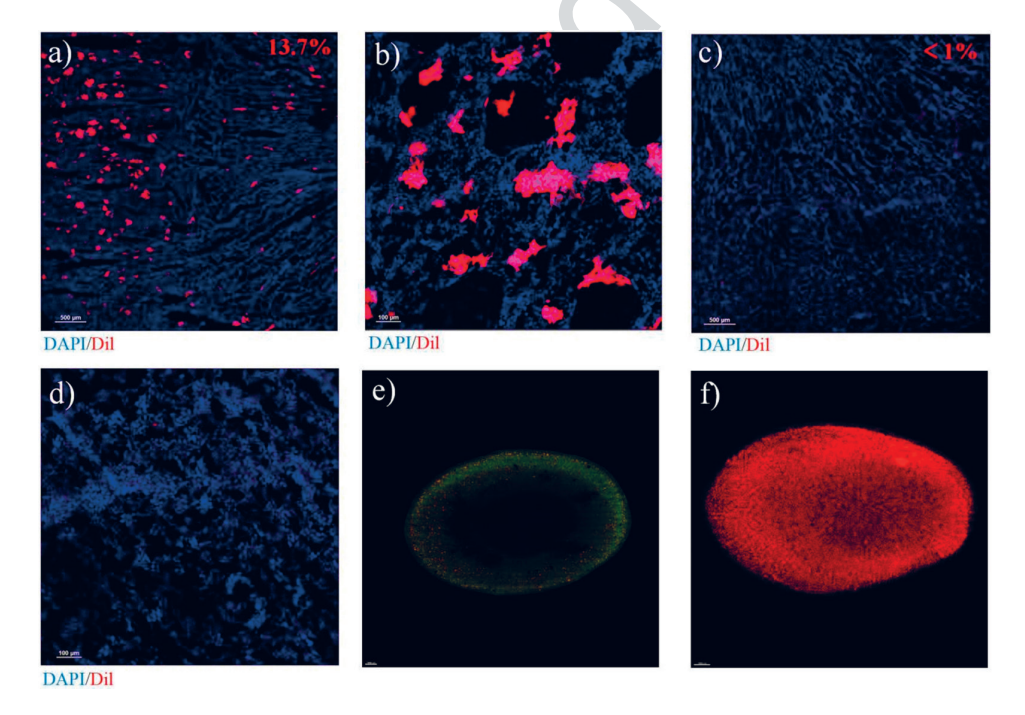


Fig. 4. Laser confocal microscopy imaging of interventional delivery of labeled UC-MSCs in rabbit kidneys: a) and b) MSC distribution in the left kidney, shown at 200× and 1000× magnification, respectively; c) and d) MSC distribution in the right kidney, shown at 200× and 1000× magnification, respectively; e) and f) GFP fluorescence images acquired in SLICE mode and coronal mode, respectively.

reaching the target tissues (33). The approach employed in this research involved the delivery of UC-MSCs directly into the left kidney via an interventional guidewire inserted through the inguinal femoral artery vasculature to the left renal artery, aided by contrast imaging utilising a contrast agent. The interventional left renal artery delivery mode significantly improved the efficiency of cell delivery in the target organ, and a cell distribution of 13 ± 0.7 % could be achieved (Figs. 4a,b), while the cell number distribution in the contralateral kidney was unaffected at < 1 % (Fig. 4c,d). In contrast to administering locally, it could minimise tissue damage and decrease the likelihood of infection. Additionally, when compared to intravenous delivery, it could significantly enhance delivery effectiveness. The increased delivery efficiency will also improve the effectiveness and safety of the treatment. Toxicity can be effectively reduced because a lower dose of cells can be effectively delivered to diseased organs and tissues (34). Previous research reported that intravenously injected human MSCs produced functional improvements in mice with myocardial infarction at least partially because cells trapped in the lungs as emboli were activated to express the anti-inflammatory factor TNF-alpha inducible protein 6 (35).

To verify whether UC-MSCs could colonise the mesenchymal layer of the kidney, cells were first stained using WGA Green Cell Membrane Fluorescent Dye to enable their visualisation and tracking. The labelled cells were then injected into experimental rabbits via intervention injection. 20 hours post-injection, the rabbits were humanely euthanised, and kidney samples were collected for imaging and analysis using the Biomapping 9000 system. The imaging results demonstrated that the injected UC-MSCs successfully traversed the circulatory system, migrated to the renal tissue, and infiltrated the mesenchymal layer through blood vessels (Fig. 4e,f). Furthermore, the fluorescence signals confirmed that a substantial number of transplanted cells had established a presence within the kidney microenvironment, indicating effective colonisation.

Distribution of UC-MSCs in the kidney via local injection

The localised injection of the left kidney refers to the injection of UC-MSCs into the renal cortex under the guidance of ultrasound imaging (Fig. 5f), where the cells are left in the kidney cortex in the form of a "closed" deposit. An autopsy conducted 20 h after localised injection of the UC-MSCs into the kidney showed that the "closed" cells partially remained at the injection site (Fig. 5a), with only a small number of cells colonizing the non-injection site areas of the same kidney (Fig. 5b). Cells also travel throughout the body with the circulatory system, and a small number of cells can reach the contralateral kidney (Fig. 5c). Cells that circulate with the bloodstream are heavily sequestered by the pulmonary vasculature (Fig. 5d). In contrast, no red fluorescently labelled cells were found in the brain (Fig. 5e). Localised injection administration has a better implantation effect than intravenous administration, such as treatment of myocardial infarction, kidney transplantation, brain injury (36-39). However, clinical applications are less frequent because they are highly invasive and introduce cells into microenvironments that are not suitable for survival (40). Similarly, in another study, vein grafting was more effective than intracranial injection in promoting the survival of cerebellar Purkinje cells in spinal cerebellar ataxia (41).

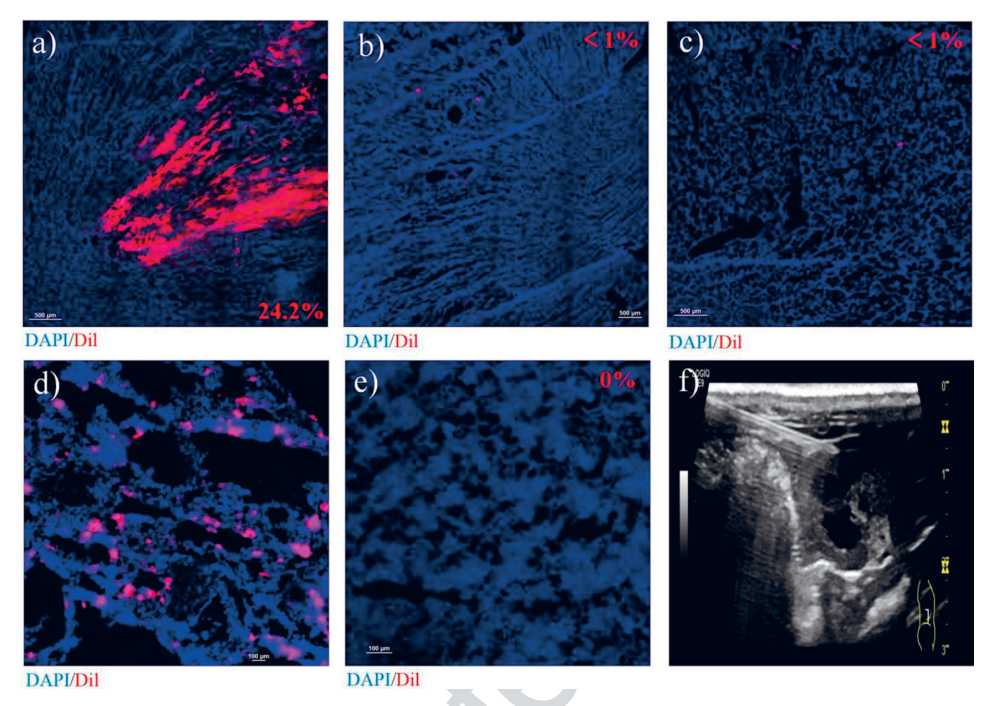


Fig. 5. Laser confocal microscopy imaging of the US-MSCs distribution in the localised injection group: a) injection site in the left kidney; b) non-injection site part in the left kidney; c) right kidney; d) pulmonary vasculature; e) brain; f) ultrasound image.

Distribution of UC-MSCs in the intravenous injection group

The findings from the autopsy conducted 20 hours post intravenous injection of UC-MSCs revealed minimal presence of red fluorescently labelled cells in the left kidney, with less than 1 % detected (Fig. 6a). Similarly, the distribution of these labelled cells in the right kidney was notably low, also less than 1 % (Fig. 6b). Conversely, a significant accumulation of red fluorescently labelled UC-MSCs was observed in the lungs (Fig. 6c). Further, no UC-MSCs were found in the brain (Fig. 6d).

The results indicate that following an intravenous injection, UC-MSCs predominantly localise in the lungs, with minimal passage to other organs (39). This lung accumulation is consistent with the "pulmonary first-pass effect" (42–44), where the cells are trapped in the lung capillary network due to their relatively large size (43, 45). In contrast, both kidneys showed very low levels (< 1 %), suggesting that these organs are not major sites of UC-MSC engraftment under these conditions (46). Furthermore, the absence of cells in the brain highlights the blood–brain barrier's role in preventing MSC entry (47, 48) (Fig. 7).

The above findings are crucial for optimising therapeutic strategies, particularly when targeting diseases of organs other than the lung, as they underscore the need for alternative delivery methods or cell modifications to enhance homing beyond the pulmonary circulation (49, 50)

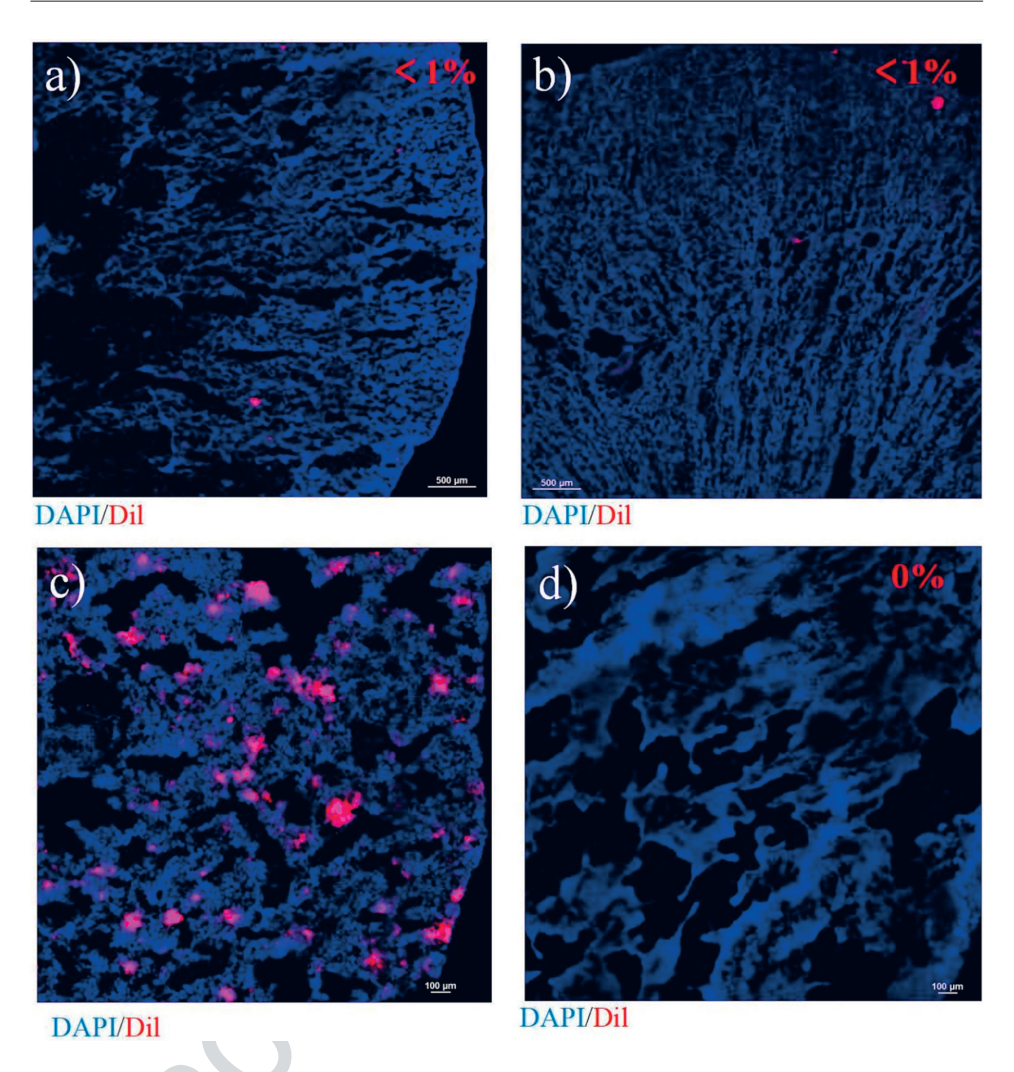
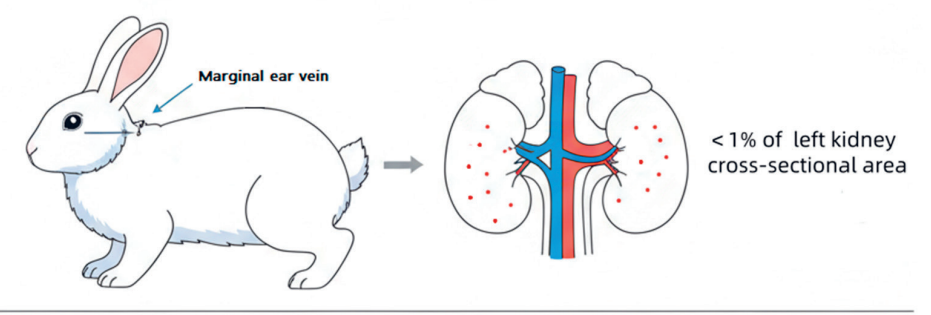


Fig. 6. Laser confocal microscope imaging of UC-MSCs in rabbit diverse organs in the intravenous injection group: a) left kidney; b) right kidney; c) lungs; d) brain.

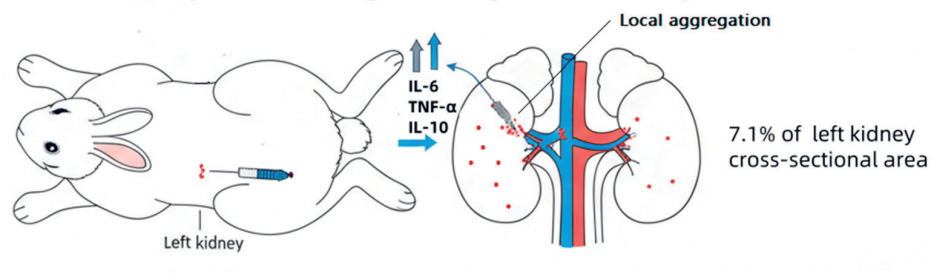
CONCLUSIONS

Local renal injection results in high MSC accumulation at the injection site, creating a pronounced difference between targeted and contralateral kidneys, but cells outside the injection site are limited and comparable to intravenous delivery. Marginal ear vein injection is simple, convenient, and highly reproducible, but yields minimal renal homing and no significant kidney-specific distribution. Interventional injection provides the most efficient and uniform renal delivery, balancing efficacy and safety. These findings underscore

a) Intravenous Injection: Low Systemic Homing



b) Local Renal Injection: Low targeted & Higher Inflammatory



c) Interventional Injection: Uniform & Efficient Delivery

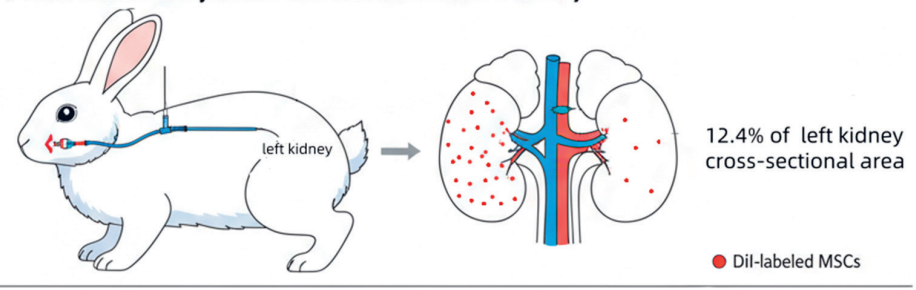


Fig. 7. The diagram illustrating the distribution of MSCs in the left and right kidneys of rabbits under three different injection methods.

that, in preclinical and clinical MSC-based therapies, careful consideration of cell source, dose, administration route, and timing is essential. The choice of delivery method should be tailored to the disease context, optimising targeted cell distribution while minimising adverse effects.

Acknowledgments. – We gratefully acknowledge the foundation support of Shenzhen Second People's Hospital Clinical Research Fund of Shenzhen High-level Hospital Construction Project (20253357011), and Research Funding for postdoctoral students who came to Shenzhen (szbo202409).

Conflict of interest. - The authors declare no conflicts of interest.

Authors contributions. – Conceptualisation, L.X., F.X., and J.L.; methodology, S.Q., Y.L., and X.W.; investigation, Y.W., Y.P., and X.Z.; data processing, C.L., F.X., H.C., and Y.L.; writing, original draft preparation, X.X., S.Q., and X.W.; writing, review and editing, L.X., X.Z., Y.W., and J.L.; supervision, J.L.; project administration, Y.W. All authors have read and agreed to the published version of the manuscript.

REFERENCES

- M. F. Pittenger, D. E. Discher, B. M. Péault, D. G. Phinney, J. M. Hare and A. I. Caplan, Mesenchymal stem cell perspective: Cell biology to clinical progress, npj Regen. Med. 4(1) (2019) Article ID 22 (15 pages); https://doi.org/10.1038/s41536-019-0083-6
- P. Wanyan, X. Wang, N. Li, Y. Huang, Y. She and L. Zhang, Mesenchymal stem cells therapy for acute kidney injury: A systematic review with meta-analysis based on rat model, *Front. Pharmacol.* 14 (2023) Article ID 1099056 (14 pages); https://doi.org/10.3389/fphar.2023.1099056
- 3. X. Han, J. Wang, R. Li, M. Huang, G. Yue, L. Guan, Y. Deng, W. Cai and J. Xu, Placental mesenchymal stem cells alleviate podocyte injury in diabetic kidney disease by modulating mitophagy via the SIRT1-PGC-1alpha-TFAM pathway, *Int. J. Molecular Sci.* 24(5) (2023) Article ID 22 (19 pages); https://doi.org/10.3390/ijms24054696
- S. Afra and M. M. Matin, Potential of mesenchymal stem cells for bioengineered blood vessels in comparison with other eligible cell sources, *Cell Tissue Res.* 380 (2020) 1–13; https://doi.org/10.1007/ s00441-019-03161-0
- Z. W. Htay, C. F. S. Ng, Y. Kim, Y.-H. Lim, M. Iwagami and M. Hashizume, Associations between short-term exposure to ambient temperature and renal disease mortality in Japan during 1979– 2019: A time-stratified case-crossover analysis, *Environmental Epidemiology* 8(1) (2024) e293 (7 pages); https://doi.org/10.1097/ee9.00000000000000293
- K. Iseri, M. Iyoda, H. Ohtaki, K. Matsumoto, Y. Wada, T. Suzuki, Y. Yamamoto, T. Saito, K. Hihara, S. Tachibana, K. Honda and T. Shibata, Therapeutic effects and mechanism of conditioned media from human mesenchymal stem cells on anti-GBM glomerulonephritis in WKY rats, Am. J. Physiol. Renal Physiol. 310(11) (2016) F1182-91; https://doi.org/10.1152/ajprenal.00165.2016
- R. J. Cheng, A. J. Xiong, Y. H. Li, S. Y. Pan, Q. P. Zhang, Y. Zhao, Y. Liu and T. N. Marion, Mesenchymal stem cells: Allogeneic MSC may be immunosuppressive but autologous MSC are dysfunctional in lupus patients, Front. Cell Dev. Biol. 7 (2019) Article ID 285 (13 pages); https://doi.org/10.3389/fcell.2019.00285
- J. Barbado, S. Tabera, A. Sánchez and J. García-Sancho, Therapeutic potential of allogeneic mesenchymal stromal cells transplantation for lupus nephritis, *Lupus* 27(13) (2018) 2161–2165; https://doi.org/10.1177/0961203318804922
- 9. H. S. Kim, J. S. Lee, H. K. Lee, E. J. Park, H. W. Jeon, Y. J. Kang, T. Y. Lee, K. S. Kim, S. C. Bae, J. H. Park and S. B. Han, Mesenchymal stem cells ameliorate renal inflammation in adriamycin-induced nephropathy, *Immune Netw.* **19**(5) (2019) e36 (10 pages); https://doi.org/10.4110/in.2019.19.e36
- N. Starc, M. Li, M. Algeri, A. Conforti, L. Tomao, A. Pitisci, F. Emma, G. Montini, P. Messa, F. Locatelli, M. E. Bernardo and M. Vivarelli, Phenotypic and functional characterization of mesenchymal stromal cells isolated from pediatric patients with severe idiopathic nephrotic syndrome, *Cytotherapy* 20(3) (2018) 322–334; https://doi.org/10.1016/j.jcyt.2017.12.001
- 11. H. H. Chang, S. P. Hsu and C. T. Chien, Intrarenal transplantation of hypoxic preconditioned mesenchymal stem cells improves glomerulonephritis through anti-oxidation, anti-ER stress, anti-inflammation, anti-apoptosis, and anti-autophagy, Antioxidants (Basel, Switzerland) 9(1) (2019); Article ID 2 (17 pages) https://doi.org/10.3390/antiox9010002

- V. A. Varela, E. B. Oliveira-Sales, E. Maquigussa, F. T. Borges, P. P. Gattai, A. D. S. Novaes, C. G. Shimoura, R. R. Campos and M. A. Boim, Treatment with mesenchymal stem cells improves renovascular hypertension and preserves the ability of the contralateral kidney to excrete sodium, *Kidney Blood Pressure Res.* 44(6) (2019) 1404–1415; https://doi.org/10.1159/000503346
- M. Gregorini, R. Maccario, M.A. Avanzini, V. Corradetti, A. Moretta, C. Libetta, P. Esposito, F. Bosio, A. Dal Canton and T. Rampino, Antineutrophil cytoplasmic antibody-associated renal vasculitis treated with autologous mesenchymal stromal cells: evaluation of the contribution of immune-mediated mechanisms, *Mayo Clinic Proc.* 88(10) (2013) 1174–1179; https://doi.org/10.1016/j.mayocp.2013.06.021
- Y. Shi, J. Xie, M. Yang, J. Ma and H. Ren, Transplantation of umbilical cord mesenchymal stem cells into mice with focal segmental glomerulosclerosis delayed disease manifestation, *Ann. Transl. Med.* 7(16) (2019) Article ID 3 (9 pages); https://doi.org/10.21037/atm.2019.07.71
- F. Yu, J. Chen, X. Wang, Q. Cai, K. Chen and Y. He, MSC-Derived exosomes prevent peritoneal fibroblast transdifferentiation in peritoneal dialysis-associated peritoneal fibrosis, Nephrol. Dialysis Transplant. 38(Supplement_1) (2023) Article ID 4662 (1 page); https://doi.org/10.1093/ndt/ gfad063c 4662
- E. Maličev and K. Jazbec, An overview of mesenchymal stem cell heterogeneity and concentration, *Pharmaceuticals* 17(3) (2024) Article ID 350 (14 pages); https://doi.org/10.3390/ph17030350
- S. Joshi, S. Allabun, S. Ojo, M. S. Alqahtani, P. K. Shukla, M. Abbas, C. Wechtaisong and H. M. Almohiy, Enhanced drug delivery system using mesenchymal stem cells and membrane-coated nanoparticles, *Molecules* 28(5) (2023) Article ID 2130 (25 pages); https://doi.org/10.3390/molecules28052130
- C. Qi, H. Shi, M. Fan, W. Chen, H. Yao, C. Jiang, L. Meng, S. Pang and R. Lin, Microvesicles from bone marrow-derived mesenchymal stem cells promote Helicobacter pylori-associated gastric cancer progression by transferring thrombospondin-2, *Cell Commun. Signal.* 21(1) (2023) Article ID 274 (15 pages); https://doi.org/10.1186/s12964-023-01127-y
- A. F. Wise, T. M. Williams, M. B. Kiewiet, N. L. Payne, C. Siatskas, C. S. Samuel and S. D. Ricardo, Human mesenchymal stem cells alter macrophage phenotype and promote regeneration via homing to the kidney following ischemia-reperfusion injury, Am. J. Physiol. Renal Physiol. 306(10) (2014) F1222-35; https://doi.org/10.1152/ajprenal.00675.2013
- S. Qi and D. Wu, Bone marrow-derived mesenchymal stem cells protect against cisplatin-induced acute kidney injury in rats by inhibiting cell apoptosis, *Int. J. Mol. Med.* 32(6) (2013) 1262–1272; https://doi.org/10.3892/ijmm.2013.1517
- M. Han, Z. Zhang, Z. Liu, Y. Liu, H. Zhao, B. Wang, C. Zhang, H. Shang, Y. Li and S. Wang, Three-dimensional-cultured MSC-derived exosome with hydrogel for cerebral ischemia repair, *Biomaterials Advan.* 149 (2023) Article ID 213396; https://doi.org/10.1016/j.bioadv.2023.213396
- C. K. Ward, R. G. Gill, R. S. Liddell and J. E. Davies, Umbilical cord stem cell lysate: a new biologic injectate for the putative treatment of acute temporomandibular joint inflammation, J. Inflamm. Res. 16 (2023) 4287–4300; https://doi.org/10.2147/R.S420741
- S. J. Lee, M. O. Ryu, M. S. Seo, S. B. Park, J. O. Ahn, S. M. Han, K. S. Kang, D. H. Bhang and H. Y. Youn, Mesenchymal stem cells contribute to improvement of renal function in a canine kidney injury model, *In vivo* 31(6) (2017) 1115–1124; https://doi.org/10.21873/invivo.11177
- 24. J. M. Quimby, T. L. Webb, D. S. Gibbons and S. W. Dow, Evaluation of intrarenal mesenchymal stem cell injection for treatment of chronic kidney disease in cats: A pilot study, *J. Feline Med. Surgery* **13**(6) (2011) 418–426; https://doi.org/10.1016/j.jfms.2011.01.005
- M. Taninokuchi Tomassoni, Y. Zhou, L. Braccischi, F. Modestino, J. Fukuda and C. Mosconi, Trans-arterial stem cell injection (TASI): The role of interventional radiology in regenerative medicine, J. Clin. Med. 13(3) (2024) Article ID 910 (13 pages); https://doi.org/10.3390/jcm13030910

- S. Levitte, A. Ganguly, S. Frolik, A. A. Guevara-Tique, S. Patel, A. Tadas, O. Klein, D. Shyr, R. Agarwal-Hashmi and L. Beach, Precision delivery of steroids as a rescue therapy for gastrointestinal graft-versus-host disease in pediatric stem cell transplant recipients, J. Clin. Med. 12(13) (2023) Article ID 4229 (6pages); https://doi.org/10.3390/jcm12134229
- 27. E. Cambria, J. Steiger, J. Günter, A. Bopp, P. Wolint, S. P. Hoerstrup and M. Y. Emmert, Cardiac regenerative medicine: The potential of a new generation of stem cells, *Transfusion Med. Hemotherapy* **43**(4) (2016) 275–281; https://doi.org/10.1159/000448179
- Y.-H. Chen, T. Xiao, X.-M. Zheng, Y. Xu, K.-T. Zhuang, W.-J. Wang, X.-M. Chen, Q. Hong and G.-Y. Cai, Local renal treatments for acute kidney injury: A review of current progress and future translational opportunities, *J. Endourology* 38(5) (2024) 466–479; https://doi.org/10.1089/end.2023.0705
- 29. R. Binato, T. de Souza Fernandez, C. Lazzarotto-Silva, B. Du Rocher, A. Mencalha, L. Pizzatti, L. F. Bouzas and E. Abdelhay, Stability of human mesenchymal stem cells during in vitro culture: considerations for cell therapy, *Cell Prolif.* **46**(1) (2013) 10–22; https://doi.org/10.1111/cpr.12002
- 30. G. Cai, Y. Lu, J. Chen, D. Yang, R. Yan, M. Ren, S. He, S. Wu and Y. Zhao, Brain-wide mapping of c-Fos expression with fluorescence micro-optical sectioning tomography in a chronic sleep deprivation mouse model, *Neurobiol. Stress* 20 (2022) Article ID 100478 (13 pages); https://doi.org/10.1016/j. ynstr.2022.100478
- 31. A. Mii, A. Shimizu, H. Yamaguchi and S. Tsuruoka, Renal complications after hematopoietic stem cell transplantation: role of graft-versus-host disease in renal thrombotic microangiopathy, *J. Nippon Med. School* 87(1) (2020) 7–12; https://doi.org/10.1272/jnms.JNMS.2020_87-102
- 32. H. Zhou, Z. Liu, Y. Wang, X. Wen, E. H. Amador, L. Yuan, X. Ran, L. Xiong, Y. Ran, W. Chen and Y. Wen, Colorectal liver metastasis: molecular mechanism and interventional therapy, *Sig. Transduct. Target. Ther.* 7(1) (2022) Article ID 70 (25 pages); https://doi.org/10.1038/s41392-022-00922-2
- 33. D. Luger, M. J. Lipinski, P. C. Westman, D. K. Glover, J. Dimastromatteo, J. C. Frias, M. T. Albelda, S. Sikora, A. Kharazi and G. Vertelov, Intravenously delivered mesenchymal stem cells: systemic anti-inflammatory effects improve left ventricular dysfunction in acute myocardial infarction and ischemic cardiomyopathy, *Circulation Res.* 120(10) (2017) 1598–1613; https://doi.org/10.1161/CIR-CRESAHA.117.310599
- 34. Y. Wang and Y. Guo, RenalGuard system and conventional hydration for preventing contrast-associated acute kidney injury in patients undergoing cardiac interventional procedures: A systematic review and meta-analysis, *Int. J. Cardiology* 333 (2021) 83–89; https://doi.org/10.1016/j.ijcard 2021 02 071
- R. H. Lee, A. A. Pulin, M. J. Seo, D. J. Kota, J. Ylostalo, B. L. Larson, L. Semprun-Prieto, P. Delafontaine and D. J. Prockop, Intravenous hMSCs improve myocardial infarction in mice because cells embolized in lung are activated to secrete the anti-inflammatory protein TSG-6, Cell Stem Cell 5(1) (2009) 54–63; https://doi.org/10.1016/j.stem.2009.05.003
- 36. S. Zonta, M. De Martino, G. Bedino, G. Piotti, T. Rampino, M. Gregorini, F. Frassoni, A. Dal Canton, P. Dionigi and M. Alessiani, Which is the most suitable and effective route of administration for mesenchymal stem cell-based immunomodulation therapy in experimental kidney transplantation: Endovenous or arterial?, *Transplant. Proc.* 42(4) (2010) 1336–1340; https://doi.org/10.1016/j. transproceed.2010.03.081
- T. Freyman, G. Polin, H. Osman, J. Crary, M. Lu, L. Cheng, M. Palasis and R. L. Wilensky, A quantitative, randomized study evaluating three methods of mesenchymal stem cell delivery following myocardial infarction, Eur. Heart J. 27(9) (2006) 1114–1122; https://doi.org/10.1093/eurheartj/ehi818
- D. Lu, Y. Li, L. Wang, J. Chen, A. Mahmood and M. Chopp, Intraarterial administration of marrow stromal cells in a rat model of traumatic brain injury, J. Neurotrauma 18(8) (2001) 813–819; https:// doi.org/10.1089/089771501316919175

- P. Walczak, J. Zhang, A. A. Gilad, D. A. Kedziorek, J. Ruiz-Cabello, R. G. Young, M. F. Pittenger, P. C. van Zijl, J. Huang and J. W. Bulte, Dual-modality monitoring of targeted intraarterial delivery of mesenchymal stem cells after transient ischemia, *Stroke* 39(5) (2008) 1569–1574; https://doi.org/10.1161/strokeaha.107.502047
- G. F. Muschler, C. Nakamoto and L. G. Griffith, Engineering principles of clinical cell-based tissue engineering, J. Bone Joint Surgery 86(7) (2004) 1541–1558; https://doi.org/10.2106/00004623-200407000-00029
- 41. Y. K. Chang, M. H. Chen, Y. H. Chiang, Y. F. Chen, W. H. Ma, C. Y. Tseng, B. W. Soong, J. H. Ho and O. K. Lee, Mesenchymal stem cell transplantation ameliorates motor function deterioration of spinocerebellar ataxia by rescuing cerebellar Purkinje cells, *J. Biomed. Sci.* 18 (2011) Article ID 54 (9 pages); https://doi.org/10.1186/1423-0127-18-54
- 42. I. M. Barbash, P. Chouraqui, J. Baron, M. S. Feinberg, S. Etzion, A. Tessone, L. Miller, E. Guetta, D. Zipori, L. H. Kedes, R. A. Kloner and J. Leor, Systemic delivery of bone marrow-derived mesenchymal stem cells to the infarcted myocardium: feasibility, cell migration, and body distribution, *Circulation* 108(7) (2003) 863–868; https://doi.org/10.1161/01.Cir.0000084828.50310.6a
- 43. S. M. Devine, A. M. Bartholomew, N. Mahmud, M. Nelson, S. Patil, W. Hardy, C. Sturgeon, T. Hewett, T. Chung, W. Stock, D. Sher, S. Weissman, K. Ferrer, J. Mosca, R. Deans, A. Moseley and R. Hoffman, Mesenchymal stem cells are capable of homing to the bone marrow of non-human primates following systemic infusion, *Exp. Hematology* 29(2) (2001) 244–255; https://doi.org/10.1016/s0301-472x(00)00635-4
- 44. J. Gao, J. E. Dennis, R. F. Muzic, M. Lundberg and A. I. Caplan, The dynamic in vivo distribution of bone marrow-derived mesenchymal stem cells after infusion, *Cells Tissues Organs* **169**(1) (2001) 12–20; https://doi.org/10.1159/000047856
- 45. S. M. Devine, C. Cobbs, M. Jennings, A. Bartholomew and R. Hoffman, Mesenchymal stem cells distribute to a wide range of tissues following systemic infusion into nonhuman primates, *Blood* **101**(8) (2003) 2999–3001; https://doi.org/10.1182/blood-2002-06-1830
- 46. J. W. Lee, X. Fang, N. Gupta, V. Serikov and M. A. Matthay, Allogeneic human mesenchymal stem cells for treatment of E. coli endotoxin-induced acute lung injury in the ex vivo perfused human lung, PNAS 106(38) (2009) 16357–16362; https://doi.org/10.1073/pnas.0907996106
- 47. G. Moll, R. Jitschin, L. von Bahr, I. Rasmusson-Duprez, B. Sundberg, L. Lönnies, G. Elgue, K. Nilsson-Ekdahl, D. Mougiakakos, J. D. Lambris, O. Ringdén, K. Le Blanc and B. Nilsson, Mesenchymal stromal cells engage complement and complement receptor bearing innate effector cells to modulate immune responses, *PloS one* 6(7) (2011) e21703 (9 pages); https://doi.org/10.1371/journal.pone.0021703
- I. U. Schraufstatter, R. G. Discipio, M. Zhao and S. K. Khaldoyanidi, C3a and C5a are chemotactic factors for human mesenchymal stem cells, which cause prolonged ERK1/2 phosphorylation, J. Immunol. 182(6) (2009) 3827–3836; https://doi.org/10.4049/jimmunol.0803055
- A. I. Caplan and D. Correa, The MSC: an injury drugstore, Cell Stem Cell 9(1) (2011) 11–15; https://doi.org/10.1016/j.stem.2011.06.008
- A. Shabbir, D. Zisa, H. Lin, M. Mastri, G. Roloff, G. Suzuki and T. Lee, Activation of host tissue trophic factors through JAK-STAT3 signaling: a mechanism of mesenchymal stem cell-mediated cardiac repair, Am. J. Physiol. Heart Circul. Physiol. 299(5) (2010) H1428-1438; https://doi.org/10.1152/ ajpheart.00488.2010